Optimal Network-Assisted Multi-user DASH Video Streaming

Emre Ozfatura, Ozgur Ercetin, Hazer Inaltekin,

arXiv:1703.03214v1 [cs.NI] 9 Mar 2017

***Abstract*—Streaming video is becoming the predominant type of traffic over the Internet with reports forecasting the video content to account for 80% of all traffic by 2019. With significant investment on Internet backbone, the main bottleneck remains at the edge servers (e.g., WiFi access points, small cells, etc.). In this work, we propose and prove the optimality of a multi-user resource allocation mechanism operating at the edge server that minimizes the probability of stalling of video streams due to buffer under-flows. Our proposed policy utilizes Media Presentation Description (MPD) files of clients that are sent in compliant to Dynamic Adaptive Streaming over HTTP (DASH) protocol to be cognizant of the deadlines of each of the media file to be displayed by the clients. Then, the policy schedules the users in the order of their deadlines. After establishing the optimality of this policy to minimize the stalling probability for a network with links associated with fixed loss rates, the utility of the algorithm is verified under realistic network conditions with detailed NS-3 simulations.**

***Index Terms*—MPEG, rebuffer, buffer starvation, quality of service, dynamic programming, playout, playback, segment**

I. Introduction

THIShere is an increasing demand for multimedia streaming applications thanks to the ubiquity of internet access, the availability of the online content and the growing number of wireless hand-held devices. The predictions of Cisco Visual Networking Index [1] indicate that IP video traffic will constitute 79 percent of all consumer internet traffic by 2018. For instance, in 2014, YouTube and Netflix account for up to 49 percent of fixed access Internet traffic in North America [2]. Moreover, 20 percent of the mobile internet traffic in North America is solely based on YouTube [2].

In this work, we propose a Dynamic Adaptive Streaming over HTTP (DASH)-compatible multi-user resource control policy called Earliest Deadline First (EDF) policy operating at an edge server. The aim of our proposed control policy is to perform scheduling of the transmission of media files so as to minimize the probability of a *stalling* event at a client. When the amount of data at the buffer of a client is insufficient to continue to display the video stream, a stalling event occurs, and the client begins a re-buffering period during which it fills its buffer without displaying the video stream. Our proposed policy utilizes Media Presentation Description (MPD) files of clients that are sent in compliant to DASH protocol to be cognizant of the deadlines of each of the media file to be displayed by the clients. Then, the policy schedules the users in the order of their deadlines. We formally prove that this policy minimizes the stalling probability for a network with links associated with fixed loss rates.

In conventional applications of DASH framework, the client is the only agent that manages the video streaming process in order to maximize the subjective video quality [3], [4], [5]. In particular, the main promise of DASH is that the clients dynamically select among different representations of the same media stream differing with respect to video encoding rates based on the estimated network throughput. However, while each client has access to only its own MDP file, the edge server has access to MDP files of all clients it is serving. Hence, the edge server has a better view of the overall operation of the network, and it is in a position to *proactively* take scheduling decisions to prevent stalling events, whereas individual clients can only react after a stalling event occurs. DASH protocol has several benefits over push-based media streaming protocols such as Real-time Transport Protocol (RTP) [6], [7], [8], [9]. First, the infrastructure of the Internet has evolved to efficiently support HTTP, and HTTP offers ubiquitous connectivity. Second, DASH is a pull-based protocol, so it traverses the firewalls. Third, the underlying TCP/IP protocol is widely deployed and provide reliable data transmission. Fourth, a client does not have to maintain a session state on the server to stream over the HTTP reducing overhead at the server.

The importance of the problem is well established as indicated by past and ongoing studies, e.g., [10] and [11]. In [10], the authors examined the joint optimization of network resource allocation and video quality adaptation. The authors propose a resource allocation algorithm that aims to prevent the stalling event by employing a parameter that reflects the risk of stalling according to the duration of the video in the clients buffer. A larger rate is assigned to a user that has a high stalling risk. In [11], the authors introduce the notion of *playout lead*, which is defined as the duration of the additional time a client can play the video by using its currently buffered data. The authors propose an algorithm that aims to prevent the stalling occurrences by maximizing the playout lead for all clients. To this end, the resource (time slots) is allocated so that the minimum of the playout lead among all users is maximized. Our work improves the current state-of-the-art in two ways. First, we prove that our proposed policy of serving the clients in the order of deadlines is optimal in the sense that it minimizes the stalling event probability of the network when the link loss rates are fixed. Second, our policy relies only on Acknowledgment (ACK) feedback from the clients

E. Ozfatura and O. Ercetin are with the Faculty of Engineering and Natural Sciences, Sabanci University, 34956 Istanbul, Turkey.

H. Inaltekin is with the Department of Electronics Engineering, International Antalya University, Antalya, Turkey.

This work is supported in part by a grant from Argela Technologies, Turkey.

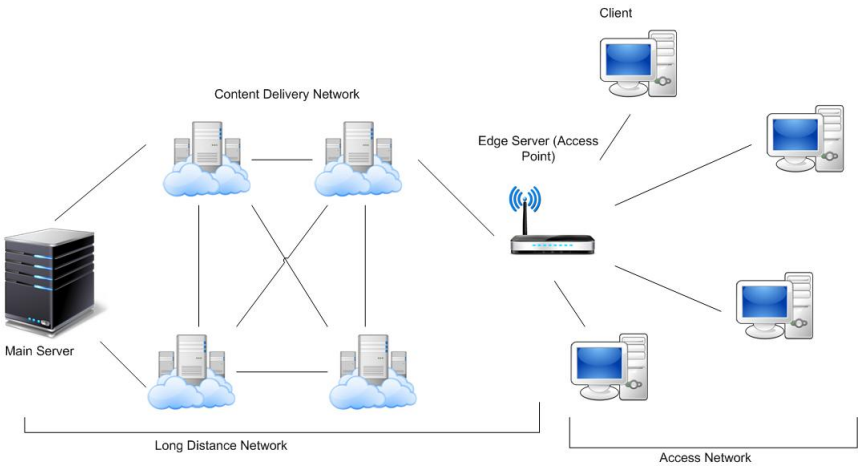

Fig. 1: Multiuser video streaming system

taken in the form of HTTP GET requests for the subsequent byte ranges of the media file, and thus, significantly reducing the implementation complexity.

The paper is organized as follows. In Section II, we provide a detailed background on the operation of DASH protocol and on the implementation of EDF as well as summarizing the current state-of-the-art and describing our contributions. Section III provides an analytical model for our system as well as the optimum scheduling problem to be solved. The definition of EDF algorithm and its optimality is given in Section IV. The implementation of the proposed algorithm is explained in Section V. The numerical analysis of EDF in comparison to a naïve but common *round-robin* scheduling algorithm is given in Section VI. Finally, we conclude with a summary of findings and future directions in Section VII.

II. Background and Related Work

A. DASH Video Streaming

As illustrated in Fig. 1, the studied video streaming system consists of two main sections: A Long Distance Network (LDN) and an Access Network (AN). The LDN may involve both a main server and a content delivery network (CDN), and it has the responsibility of delivering the requested video files to the edge servers in the AN. In general, the bottleneck of the end-to-end connection is at the edge servers, so we focus on the resource allocation strategies operating at the edge servers to alleviate this bottleneck.

Due to their significant advantages over push-based media streaming protocols such as RTP, HTTP-based streaming protocols have been widely adopted by most of the on-demand video service providers. In particular, DASH protocol is developed to provide a common set of functionality among different HTTP-based streaming protocols [6], [7], [8], [9].

In DASH, a video file is encoded with multiple different bitrates into different *representations*, where each representation corresponds to a different level of quality of the same video stream. Each representation is broken into *Segments* of duration 2-10 seconds [12]. Segments may be further subdivided into *Sub-segments*, each of which contains a whole number of complete access units. The video content providers employing DASH often use video files encoded according to Advanced Video Coding (AVC) (e.g., H264.AVC) standard. In this video encoding format, the smallest meaningful bit-chunk is called *Group of Pictures* (GoP) since the frames of the same GoP are encoded and decoded together [13], [9]. Thus, an AVC encoded video file is considered as a combination of mutually exclusive fragments that contain different frames of the same video file. Each GoP contains a fixed number of frames and has a fixed video display duration. We note that although each GoP has a fixed video display duration, their sizes might be different due to video content. To display a frame, all information related to the corresponding GoP needs to be available at the client buffer. The DASH client behavior can be summarized as follows. The client first accesses the Media Presentation Description (MPD) file. The MPD file contains metadata required by a DASH client to construct appropriate HTTP-URLs to access Segments and to provide the streaming service to the user. In particular, an MPD file provides information for the earliest presentation time and presentation duration for each segment in the representation[1]. The client selects an appropriate video representation (typically based on an estimate of the available bandwidth to the server but also on the rendering capabilities of the client). Then, the client creates a list of accessible Segments for each representation. The client accesses the content by requesting entire Segments or byte ranges of Segments via HTTP-GET command. Once the presentation has started, the client continues consuming the media content by continuously requesting Segments or parts of Segments. The client may switch representations taking into account updated information from its environment, e.g., change of observed throughput. In our proposed framework, we focus on the scheduling and resource allocation at the edge server, so DASH clients may use any adaptive video quality selection algorithm to select an appropriate representation based on the observed throughput and client capabilities.

[1]This information will be used by our proposed algorithm to perform resource allocation among multiple DASH clients.

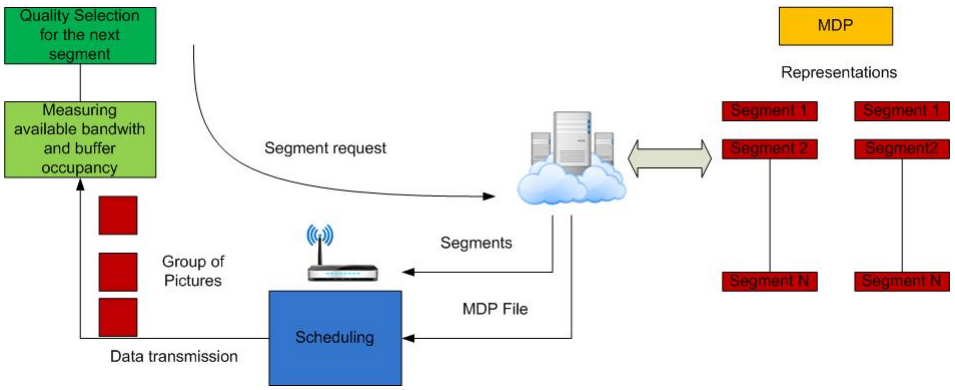

Fig. 2: End-to-end video streaming system.

B. Related Work

There is a plethora of work on the adaptation of quality of video with respect to the network conditions. In particular, many prior studies investigate the use of scalable video coding (SVC) for this purpose[14], [15], [16], [17], [18], [19]. In almost all of these works, a rate-distortion metric is first constructed by considering the specific structure of the video. Then, a utility function which is defined with respect to this metric is optimized by developing different scheduling, rate allocation, and admission control policies. Although there is still an ongoing interest on the use of SVC along side DASH [20], in most commercial applications this alternative is forgone, mainly because SVC requires a control mechanism at the server side that introduces an added complexity contradicting with the initial premise of the DASH structure.

In [21], [22], [23], the process of video streaming over HTTP is explained in detail and the specifications of the DASH protocol are introduced. The rate-adaptation mechanisms of commercial players are investigated in [24]. After the standardization of DASH protocol, a great deal of attention is devoted to the client side control algorithms for bit-rate (quality) selection in order to maximize the video quality, and to minimize the fluctuations in quality and the number of stalling events [3], [4], [5]. The main purpose of all these client centric algorithms is to adjust the video source rate of users according to available resource in order to prevent congestion and corresponding stalling events. However, in our work we concentrate on the time period between the two bit-rate selection instants and show that it is possible to reduce the number of stalling events further via implementing an additional low-complexity scheduling algorithm at the server side.

It is reported that client-side approaches give rise to other problems due to over/under-estimation of the actual available bandwidth. In [25] and [26], the authors have identified three main performance issues: (i) player instability, (ii) unfairness between the players and (iii) the under-utilization of the available bandwidth. It is pointed out that the main cause of these performance issues is the successive activity and inactivity periods which leads to miscalculation of the available bandwidth. In line of this work, other studies have investigated the efficient and fair utilization of the available bandwidth [27], [28], [29].

In [27], two control mechanisms are implemented at the client side; one for controlling the playout buffer, and one for selecting the appropriate video quality level that matches the best-effort bandwidth. Furthermore, two actuators are implemented at the server; one changing the video quality, and the other throttling the video streaming rate. The fairness issues are addressed in [28] and [29]. In [28], the authors aim to adjust the rate of each segment to eliminate the off-periods (time period during which the client stops requesting a video segment). It was conjectured that the elimination of the off-periods improves the accuracy of TCP-based bandwidth estimation procedures. In [29], a randomized segment scheduler is used to prevent the problem of overestimation/underestimation of the available bandwidth due to a biased view of the network state. Proposed algorithms in [28] and [29] aim to regulate segment requests of the users in order to increase accuracy of the resource estimation process, and unlike our method introduced in the paper, these approaches are client centric. A server centric implementation also exists in [27], however the proposed control mechanism tracks the client buffers which requires an additional feedback mechanism whereas our proposed model co-operates with DASH protocol without requiring an additional feedback system.

III. Analytical Model, Definitions and the Optimum Scheduling Problem

In this section, we will introduce the details of our analytical model (following the standard terminology of the *stochastic control* literature [30]), the definitions that go with this model and the *optimum scheduling problem* that we solve to minimize the number of stalling events in DASH based multiuser video streaming systems.

A. Receiver and Playout Curves

The arrival process of client i is denoted by $R_i(t)$, which we call the *receiver curve* of client i. The receiver curve $R_i(t)$ indicates the total amount of error free data in unit of packets that is delivered to client i up to time t. For each client i, $R_i(t)$ is a non-decreasing function of t. The video of client i is displayed according to $p_i(t)$, which is called the *playout curve*. The playout curve describes the minimum amount of

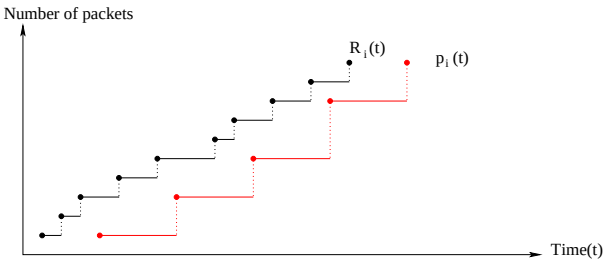

Fig. 3: Receiver and Playout curves

data in units of packets that needs to be decoded up to time t to perform uninterrupted video display. The GoP based structure of the video files implies that all playout curves are right continuous functions as illustrated by Fig. 3. A time instant $t > 0$ at which there is a jump in the playout curve, i.e., $p(t^-) \neq p(t)$ for any $t^- < t$, is called an *increment point*.

We consider a time-slotted video streaming system with fixed slot length equal to Δ so that the edge server can serve only one user in each slot duration. Hence, the receiver curve $R_i(t)$ increases by one unit at the end of a time-slot if and only if user i is scheduled at the beginning of the corresponding time-slot and the transmitted packet is received successfully. As a result of this operation, all receiver curves are right continuous functions as well, an example of which is illustrated in Fig. 3. We further assume that GoP duration is also an integer multiple of the slot duration Δ. Since both playout curves and receiver curves remain constant during a slot duration, we can discretize these functions and use time index $k = \lfloor t/\Delta \rfloor$, where $\lfloor \cdot \rfloor$ is the *floor* function that produces the largest integer smaller than or equal to its argument. Throughout the paper, we will normalize Δ to *one* time unit to simplify notation. To ensure continuous displaying of a video at client i, there should be sufficient number of packets in the client buffer so that the following inequality holds

$$R_i(t) \geq p_i(t) \tag{1}$$

for any time instant t.

B. Analytical Model and Definitions

Our primary aim is to discover the structure of the optimum scheduling policy (on the edge server side) that will minimize the stalling event probability for multiuser video streaming over stochastically varying wireless channels. To this end, we focus on minimizing the stalling probability per segment, where each segment spans $T \in \mathbb{N}$ consecutive slots of time.[2] Hence, without loss of generality, we model our optimum scheduling problem as a *finite* horizon stochastic dynamic programming problem over time interval $[0, T]$ below.

The classical packet *erasure* channel is used to model wireless channels between the end users and the edge server, as such a packet scheduled for user i is either successfully received with probability β_i or lost with probability $1 - \beta_i$ in each time slot. We assume that channel statistics $\boldsymbol{\beta} = (\beta_1, \ldots, \beta_N)$ are known at time $t = 0$ and remain the same over the time interval $[0, T]$. Similarly, we also assume that playout curves (or, alternatively called representation levels) $\boldsymbol{p}(t) = (p_1(t), \ldots, p_N(t))$ are known by the edge server at time $t = 0$, which is a standard assumption of the DASH protocol. Here, $\boldsymbol{p}(t)$ is a vector valued function that describes the amount of data (measured in terms of number of packets) required by each user up to time t to display its video without any interruptions.

The edge server can serve *only one* user in each time slot. Hence, a scheduling decision must be made at the beginning of each time slot to select an *appropriate* user (i.e., usually the one that optimizes the system performance) for data transmission based on the current system state that summarizes the data reception history. In this paper, we represent the system states by the N dimensional vector $\boldsymbol{s} = (s_1, \ldots, s_N)$, where s_i is equal to the number of packets received by user $i \in \{1, \ldots, N\}$. We will often use states with time index $\lfloor t \rfloor$ (or, by using the discrete time index $k \in \{0, \ldots, T-1\}$), i.e., $\boldsymbol{s}_{\lfloor t \rfloor} = \left(s_{1,\lfloor t \rfloor}, \ldots, s_{N,\lfloor t \rfloor}\right)$, to denote the number of packets received by the users at the beginning of time slot $\lfloor t \rfloor$. The set $\mathcal{S} = \{0, 1, 2, \ldots, T\}^N$ defines the set of all state vectors.[3]

In this setting, we define the *action set* $\mathcal{A}$ to be $\mathcal{A} = \{1, 2, \ldots, N\}$, and each action a belonging to $\mathcal{A}$ denotes the index of the user scheduled for video streaming in the current time-slot. We note that $\mathcal{A}$ is a state-independent action set that remains the same for all $\boldsymbol{s} \in \mathcal{S}$. Consider now a specific time-slot k. An important quantity of interest that describes how the video streaming system in question evolves in time is the *transition probability function* $P_k(\boldsymbol{z}|\boldsymbol{s}, a)$ that represents the transition probability of the video streaming system to another system state $\boldsymbol{z}$ at the beginning of the next time-slot given that the system state in the current time-slot k is $\boldsymbol{s}$, i.e., $\boldsymbol{s}_k = \boldsymbol{s}$, and the action taken in this time-slot is a. Using the wireless channel model between the edger server and the users, $P_k(\boldsymbol{z}|\boldsymbol{s}, a)$ can be more formally written as

$$P_k(\boldsymbol{z}|\boldsymbol{s}, a) = \begin{cases} 1 - \beta_a & \text{if } \boldsymbol{z} = \boldsymbol{s} \\ \beta_a & \text{if } \boldsymbol{z} = (s_1, \ldots, s_a + 1, \ldots, s_N) \\ 0 & \text{otherwise} \end{cases}.$$

In addition to the analytical framework introduced above, two other major components of our model that operate on this framework are *decision rules* and the *scheduling policy*, which are what we define next. Considering the fact that packet success or failure events are independent from time-slot to time-slot in our wireless channel model[4], knowledge of the current system state is sufficient to predict current channel conditions and to construct remaining playout curves, i.e., remaining demand for data for uninterrupted video streaming. Hence, without loss of generality, we focus on Markovian and

[2]The main reason for us to consider *only* the segment stalling probability in this paper is the technological constraint introduced by the DASH protocol. In particular, the DASH protocol determines the representation level of the next segment only after the current segment requests are provisioned, and we cannot state our optimum scheduling problem without knowing the representation levels of the forthcoming segments.

[3]We note that $\mathcal{S}$ is larger than the set of all admissible states. If needed to be more precise, we can write $\mathcal{S}' = \left\{\boldsymbol{s} \in \mathcal{S} : \sum_{i=1}^N s_i \leq T\right\}$.

[4]This assumption implies that knowing the transmission history and associated success or failure events do not give us any information about the channel conditions in the current time-slot.

deterministic decision rules defined as functions that map the set of states $\mathcal{S}$ to the set of actions $\mathcal{A}$. More specifically, the decision rule d_k for time-slot k takes the system state $\boldsymbol{s}_k$ in the beginning of this time-slot as an input, and produces an action a belonging to $\mathcal{A}$, i.e., $d_k(\boldsymbol{s}_k) = a \in \mathcal{A}$, that represents the user index scheduled for video streaming in this time-slot.

Utilizing the definition of decision rules, we next state the definition of scheduling policy and *tail* scheduling policy below, which will conclude the description of our analytical model.

Definition 1: A scheduling policy $\boldsymbol{\pi} = (d_0, \ldots, d_{T-1})$ is a sequence of decision rules as such the kth element of $\boldsymbol{\pi}$ determines the index of the user scheduled for the kth time-slot based on the observed system state at the beginning of this time-slot for $k \in \{0, \ldots, T-1\}$. Similarly, a tail scheduling policy $\boldsymbol{\pi}_k = (d_k, \ldots, d_{T-1})$ is a sequence of decision rules that determines the indices of the users scheduled for the time-slots from k to $T-1$.

C. The Optimum Scheduling Problem

Having introduced our analytical model above, we are now ready to state the optimum scheduling problem. To this end, we first need to define *total expected reward* that is obtained when the scheduling policy $\boldsymbol{\pi} = (d_0, \ldots, d_{T-1})$ is employed to determine scheduling decisions for each time slot.

Definition 2: The total expected reward $u_k^{\boldsymbol{\pi}} : \mathcal{S} \mapsto \mathbb{R}$ collected from time-slot k to $T-1$ under the scheduling policy $\boldsymbol{\pi} = (d_0, \ldots, d_{T-1})$ is a function that maps the initial system state $\boldsymbol{s}_k$ at the beginning of the time-slot k to a real number.

We note that $u_k^{\boldsymbol{\pi}}$ can be easily expressed recursively as

$$u_k^{\boldsymbol{\pi}}(\boldsymbol{s}_k) = r_k(\boldsymbol{s}_k, a) + \sum_{\boldsymbol{s} \in \mathcal{S}} P_k(\boldsymbol{s} | \boldsymbol{s}_k, a)\, u_{k+1}^{\boldsymbol{\pi}}(\boldsymbol{s}) \qquad (2)$$

for any $\boldsymbol{s}_k \in \mathcal{S}$, where $r_k(\boldsymbol{s}_k, a)$ denotes the reward obtained by the scheduling decision $a = d_k(\boldsymbol{s}_k)$ at time-slot k if the current system state is $\boldsymbol{s}_k$, and the summation term in (2) represents the total expected reward obtained from time-slot $k+1$ onwards. It should be noted that $u_k^{\boldsymbol{\pi}}(\boldsymbol{s}_k)$ in (2) depends on $\boldsymbol{\pi}$ only through its tail policy $\boldsymbol{\pi}_k = (d_k, \ldots, d_{T-1})$. For the sake of completeness, we set $u_T^{\boldsymbol{\pi}}(\boldsymbol{s}_T) = r_T(\boldsymbol{s}_T)$, where it is understood that $\boldsymbol{s}_T$ is the system state reached at the end of the video segment of interest, $r_T(\boldsymbol{s}_T)$ is the reward collected due to the occurrence of $\boldsymbol{s}_T$, and no action is allowed at this termination time, which is a standard assumption of the finite horizon stochastic control problems [30]. The notion of *optimality* for a scheduling policy is introduced in the following definition.

Definition 3: Let Π be the set of all scheduling policies. Then, we say that a scheduling policy $\boldsymbol{\pi}^\star$ is *optimum* if it solves the optimization problem below

$$\max_{\boldsymbol{\pi} \in \Pi} u_k^{\boldsymbol{\pi}}(\boldsymbol{s}) \qquad (3)$$

for all time-slots $k \in \{0, \ldots, T-1\}$ and initial state vectors $\boldsymbol{s} \in \mathcal{S}$.[5]

[5]The maximum value in (3) is always achieved since Π is a finite set, and hence there is no ambiguity in this definition.

We note that the condition of optimality introduced in Definition 3 is a strong one since we do not only want a given scheduling policy is optimum itself considering time-slots from 0 to $T-1$ but also want all of its tail policies to be optimum and achieve the *best* possible total expected reward starting from any time-slot and initial system state. To put it in another way, we want an optimal scheduling policy $\boldsymbol{\pi}^\star$ to satisfy the following equality

$$u_k^{\boldsymbol{\pi}^\star}(\boldsymbol{s}) = u_k^\star(\boldsymbol{s}) \qquad (4)$$

for all $k \in \{0, \ldots, T-1\}$ and $\boldsymbol{s} \in \mathcal{S}$, where $u_k^\star(\boldsymbol{s}) = \max_{\boldsymbol{\pi} \in \Pi} u_k^{\boldsymbol{\pi}}(\boldsymbol{s})$.

We will derive the structure of $\boldsymbol{\pi}^\star$ by considering a specific but practically relevant total expected reward function, which is the system-wise segment *non*-stalling probability, i.e., none of the users experiences stalling throughout a particular segment duration. Indeed, our problem formulation lends itself to readily calculate the segment non-stalling probability if we set the per-slot reward functions $r_k(\boldsymbol{s}, a)$ to zero for all $k \in \{0, \ldots, T-1\}$, set $r_T(\boldsymbol{s}_T)$ to zero (one) if a stalling event does (not) occur at the end of time-slot $T-1$ (i.e., the termination time).[6] Accordingly, the total expected reward in (2) for the segment stalling probability can be written as

$$u_{\lfloor t \rfloor}^{\boldsymbol{\pi}}(\boldsymbol{s}_{\lfloor t \rfloor}) = \begin{cases} \sum_{\boldsymbol{s} \in \mathcal{S}} P_{\lfloor t \rfloor}(\boldsymbol{s} | \boldsymbol{s}_{\lfloor t \rfloor}, a)\, u_{\lfloor t \rfloor + 1}^{\boldsymbol{\pi}}(\boldsymbol{s}) & \text{if } \boldsymbol{s}_{\lfloor t \rfloor} \succeq \boldsymbol{p}(t) \\ 0 & \text{otherwise} \end{cases}, \qquad (5)$$

where "$\succeq$" represents element-wise vector inequality and a is the action taken in time-slot $\lfloor t \rfloor$ by the scheduling policy $\boldsymbol{\pi} = (d_0, \ldots, d_{T-1})$, i.e., $a = d_{\lfloor t \rfloor}(\boldsymbol{s}_{\lfloor t \rfloor})$. It should be noted that a given scheduling policy $\boldsymbol{\pi}$ induces a probability distribution over the set of system states $\mathcal{S}$, which in turn determines a probability distribution for *random* receiver curves $R_i(t)$ for $i \in \{1, \ldots, N\}$ and $t \in [0, T]$. Hence, $u_{\lfloor t \rfloor}^{\boldsymbol{\pi}}(\boldsymbol{s}_{\lfloor t \rfloor})$ can also be written as the probability that all random receiver curves to be above all playout curves over the time interval $[t, T]$ starting from the initial system state $\boldsymbol{s}_{\lfloor t \rfloor}$. That is, $u_{\lfloor t \rfloor}^{\boldsymbol{\pi}}(\boldsymbol{s}_{\lfloor t \rfloor})$ is equal to

$$F_{\lfloor t \rfloor}(\boldsymbol{p}, \boldsymbol{\pi}_{\lfloor t \rfloor}, \boldsymbol{s}_{\lfloor t \rfloor}) = \mathsf{Pr}\left(\bigcap_{i=1}^{N} \{R_i(\tau) \geq p_i(\tau), \forall \tau \in [t, T]\} \,\middle|\, \boldsymbol{s}_{\lfloor t \rfloor} \right). \qquad (6)$$

Above representation of $u_k^{\boldsymbol{\pi}}(\boldsymbol{s})$ in (6) that shows the dependence of segment stalling (or, non-stalling to this effect) probability on receiver and playout curves explicitly will be helpful in our derivation to determine the structure of the optimum scheduling policy in the next section.

IV. The Optimum Scheduling Policy

In this section, we derive the structure of the optimum scheduling policy that solves the optimum scheduling problem introduced in Section III for maximizing the non-stalling

[6]The condition to check if a stalling event occurs or not at the end of time-slot $T-1$ is equivalent to checking the inequality $s_{i,T} \geq p_i(T)$ for all $i \in \{1, \ldots, N\}$. If this inequality is not satisfied for a user, we say that a stalling event occurs at the termination time T.

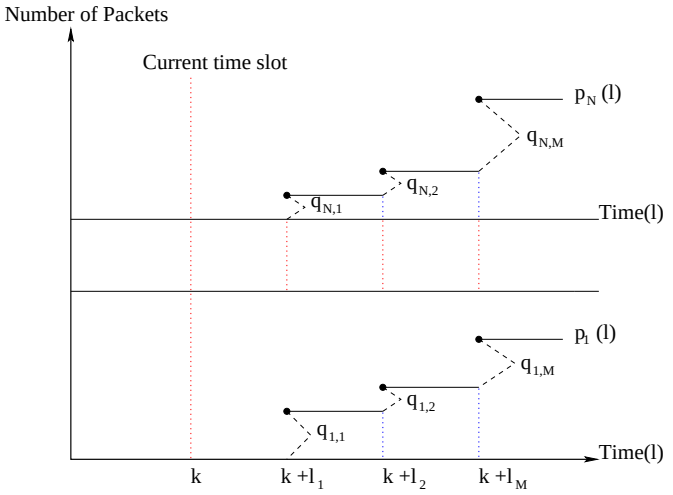

Fig. 4: Schematic representation of playout curves at the beginning of time-slot k.

event probability in multiuser video streaming systems. In particular, it will be shown that a simple but practical greedy algorithm that schedules users based on their packet deadlines maximizes the segment non-stalling probability $u_k^{\boldsymbol{\pi}}(\boldsymbol{s})$ for all initial system states $\boldsymbol{s} \in \mathcal{S}$ as well as for time-slots $k \in \{0,\ldots,T-1\}$. We call this algorithm the *earliest deadline first* (EDF) algorithm. Before we formally state the optimality of the EDF algorithm in Theorem 1, which is the main analytical result of this paper, it would be helpful to explain the operational details of the EDF algorithm through a particular situation for facilitating the upcoming discussion and the exposition of the proof of its optimality.

To this end, consider the case where the current time-slot index is k and assume that there are M jumps in the playout curves of users at time-slots $k+l_1,\ldots,k+l_M$, which is illustrated in Fig. 4. These are the ordered time instants increasing from the smallest one to the biggest one with the last time instant $k+l_M$ coming no later than T. We recall that such a jump occurring in the playout curve of a user corresponds to the additional data demanded by this user (in terms of number of packets) for smooth displaying of its video, and this data demand must be provisioned by the edge server in order to avoid video stalling at this user.

We let $q_{i,m}$ denote the height of the jump at time-slot $k+l_m$ occurring at the playout curve of user i. Here, $q_{i,m}$ corresponds to the number of additional data packets requested by user i between the deadlines $m-1$ and $m \leq M$. Therefore, we can consider the delivery of $q_{i,m}$ packets to user i as a *task* with a *deadline* $k+l_m$. If this task is accomplished by the edge server for all deadlines, then no stalling event occurs at user i. The EDF algorithm simply prioritizes all such tasks based on their deadlines by instructing the edge server to conclude the tasks with the earliest deadlines first before proceeding to those with deadlines coming at later times. If there are two or more users with the same deadline, the EDF algorithm can schedule any one of such users without any loss of optimality, and we assume that it schedules the user having the smallest index in our particular implementation of the EDF algorithm in Theorem 1.

Theorem 1: For given playout curves $\boldsymbol{p}$ and channel statistics $\boldsymbol{\beta}$, the EDF algorithm produces an optimal scheduling policy $\boldsymbol{\pi}^{edf}$ i.e.,

$$u_k^{\boldsymbol{\pi}^{edf}}(\boldsymbol{s}) = u_k^{\star}(\boldsymbol{s}) \tag{7}$$

holds for all $k=0,\ldots,T-1$ and $\boldsymbol{s} \in \mathcal{S}$.

Proof: We will prove this theorem by induction.

Base Case: We first consider the base case in which the optimum scheduling problem is solved for the last time-slot $T-1$. If there are two or more deadlines in the beginning of time-slot $T-1$, no scheduling policy can achieve stalling-free video streaming for all users, and therefore all scheduling policies are the same in terms of their segment stalling probability performances in such cases. On the other hand, if there is only one deadline in the beginning of time-slot $T-1$, the user associated with this deadline must be served to avoid a possible stalling event. This discussion shows that the EDF algorithm minimizes the segment stalling probability for the last time-slot.

Induction Step: Secondly, we consider a time-slot with index $k+1 \leq T-2$ and assume that $u_{k+1}^{\boldsymbol{\pi}^{edf}}(\boldsymbol{s}) = u_{k+1}^{\star}(\boldsymbol{s})$ for all $\boldsymbol{s} \in \mathcal{S}$. Then, it is well-known from [30] that the optimal scheduling decision for time-slot k must satisfy the following condition

$$d_k^{\star}(\boldsymbol{s}_k) \in \underset{a\in\mathcal{A}}{\operatorname{argmax}} \left\{ \sum_{\boldsymbol{s}\in\mathcal{S}} P_k(\boldsymbol{s}|\boldsymbol{s}_k,a)\, u_{k+1}^{\star}(\boldsymbol{s}) \right\} \tag{8}$$

for all system states $\boldsymbol{s}_k \in \mathcal{S}$ in the beginning of time-slot k. Since the induction hypothesis asserts that $u_{k+1}^{\boldsymbol{\pi}^{edf}}(\boldsymbol{s}) = u_{k+1}^{\star}(\boldsymbol{s})$, (8) can also be expressed as

$$d_k^{\star}(\boldsymbol{s}_k) \in \underset{a\in A}{\operatorname{argmax}} F_k\left(\boldsymbol{p}, \left(a, \boldsymbol{\pi}_{k+1}^{edf}\right), \boldsymbol{s_k}\right). \tag{9}$$

Note that the term $\left(a, \boldsymbol{\pi}_{k+1}^{edf}\right)$ in (9) is a tail scheduling policy that is obtained by concatenating an action a and the tail policy $\boldsymbol{\pi}_{k+1}^{edf}$. Next, we will show that $\boldsymbol{\pi}_k^{edf} = \left(d_k^{\star}, \boldsymbol{\pi}_{k+1}^{edf}\right)$. To this end, we will provide an alternative expression for $F_k(\boldsymbol{p},\boldsymbol{\pi}_k,\boldsymbol{s}_k)$ for any tail scheduling policy $\boldsymbol{\pi}_k$. Let there be M deadlines at $k+l_1,\ldots,k+l_M$ for a given playout curve $\boldsymbol{p}$ and system state $\boldsymbol{s}_k \in \mathcal{S}$ after the time-slot k, an example of which is illustrated in Fig. 4. Let also the random variable λ_m denote the first time-slot when all packets belonging to the first m deadlines are delivered successfully. We note that λ_m depends on the tail scheduling policy $\boldsymbol{\pi}_k$ and $\boldsymbol{p}$, and $F_k(\boldsymbol{p},\boldsymbol{\pi}_k,\boldsymbol{s}_k)$ can be expressed in terms of $\{\lambda_m\}_{m=1}^{M}$ as

$$F_k(\boldsymbol{p},\boldsymbol{\pi}_k,\boldsymbol{s}_k) = \mathsf{Pr}\left(\bigcap_{m=1}^{M} \{\lambda_m \leq k+l_m\} \,\middle|\, \boldsymbol{s}_k \right). \tag{10}$$

Consider now the random variable τ_m, which denotes the total number of time-slots required to send all $\sum_{i=1}^{N} q_{i,m}$ packets associated with the deadline at $k+l_m$ successfully. Under the EDF algorithm, the relationship between λ_m and $\{\tau_i\}_{i=1}^{m}$ is $\lambda_m = k + \sum_{i=1}^{m}\tau_i$. Hence, using (10), we obtain

$$F_k\left(\boldsymbol{p},\boldsymbol{\pi}_k^{edf},\boldsymbol{s}_k\right) = \mathsf{Pr}\left(\bigcap_{m=1}^{M} \left\{ \sum_{i=1}^{m} \tau_i \leq l_m \right\} \,\middle|\, \boldsymbol{s}_k \right). \tag{11}$$

Assume now that we choose an action $a \neq d_k^{edf}(\boldsymbol{s}_k)$ and form a tail scheduling policy $\left(a, \boldsymbol{\pi}_k^{edf}\right)$. For this tail scheduling policy, we will show that $F_k\left(\boldsymbol{p}, \left(a, \boldsymbol{\pi}_{k+1}^{edf}\right), \boldsymbol{s}_k\right) \leq F_k\left(\boldsymbol{p}, \boldsymbol{\pi}_k^{edf}, \boldsymbol{s}_k\right)$. Let the scheduled user a has the first deadline at $k + l_j$ for some $j \geq 2$. Since time-slot k is allocated for user a, and users are scheduled according to the tail policy $\boldsymbol{\pi}_{k+1}^{edf}$ in the remaining time slots, we can write $F_k\left(\boldsymbol{p}, \left(a, \boldsymbol{\pi}_{k+1}^{edf}\right), \boldsymbol{s}_k\right)$ as

$$F_k\left(\boldsymbol{p}, \left(a, \boldsymbol{\pi}_{k+1}^{edf}\right), \boldsymbol{s}_k\right) = \mathsf{Pr}\left(\bigcap_{m=1}^{M}\left\{\sum_{i=1}^{m}\tau_i \leq l_m - 1_{\{m<j\}}\right\} \,\middle|\, \boldsymbol{s}_k\right), \quad (12)$$

where $1_{\{m<j\}}$ is an indicator function that returns 1 if the inequality $m < j$ holds.[7] Comparing (11) and (12), we conclude that $F_k\left(\boldsymbol{p}, \boldsymbol{\pi}_k^{edf}, \boldsymbol{s}_k\right) \geq F_k\left(\boldsymbol{p}, \left(a, \boldsymbol{\pi}_{k+1}^{edf}\right), \boldsymbol{s}_k\right)$ for any $a \in \mathcal{A}$. This result implies that $\boldsymbol{\pi}_k^{edf}$ is the optimum tail scheduling policy starting from any time-slot k onwards, and hence $\boldsymbol{\pi}^{edf}$ is the solution of the optimum scheduling problem given by (3). ∎

An important corollary of Theorem 1 is that the optimum scheduling policy minimizing the segment stalling probability does not depend on the statistical knowledge $\boldsymbol{\beta} = (\beta_1, \ldots, \beta_N)$ of the wireless channel between the edge server and the users. This observation may seem counter-intuitive at a first glance. In particular, it can be conjectured that we should always perform better if we take channel statistics into account while giving scheduling decisions in each time-slot. However, the particular solution constructed for the optimum scheduling problem in Theorem 1, i.e., the EDF algorithm, shows that we cannot improve the segment stalling probability even if we utilize the statistical channel knowledge.[8] The point here is that the dynamic playout curve updating procedure embedded in the EDF algorithm already includes the effect of the packet drop probabilities of the users, and this is sufficient to make the EDF algorithm an optimum scheduling policy for multiuser video streaming systems.

This observation has some important practical ramifications. Firstly, the implementation of the EDF algorithm avoids any channel estimation issues to learn channel conditions before it starts its operation. In particular, implementation of a channel estimation algorithm suited for the particular requirements of video streaming coupled with an efficient and high-throughput feedback protocol design (for frequency-division-duplexing systems) from users to the edge server may become an onerous task for delay sensitive video traffic.

Secondly, perhaps the most importantly, the EDF algorithm is proposed as an *add-on* solution to the existing video streaming systems, especially to the DASH based systems, for improving their scheduling efficiency. Therefore, it must be backward-compatible with them for all practical purposes, rather than necessitating a substantial re-design of a video streaming system. Besides improving the scheduling efficiency of video streaming systems by minimizing the stalling event probability, its simple and channel statistics invariant nature makes the EDF algorithm an ideal backward-compatible solution for serving this purpose. Finally, the EDF algorithm has only polynomial-time computational complexity due to ordering of packet deadlines, and hence easy to execute in real-time. In the next section, we present a particular NS-3 implementation of the EDF algorithm integrated into a DASH based video streaming system to illustrate its aforementioned benefits.

[7]The random variables appearing in (11) and (12) must be considered to be equal in distribution.

[8]The solution for the optimum scheduling problem in (3) is not necessarily unique, and there may exist other scheduling policies utilizing wireless channel statistics and achieving the same performance with the EDF algorithm. The determination of the complete solution set for (3) is outside the scope of the current paper.

V. Implementation

Another important corollary of Theorem 1 is that the optimum scheduling policy minimizing the segment stalling probability does not begin serving another video client before completing the transmission of a GOP of the current client. This is because, the optimal EDF algorithm serves packets in the order of upcoming deadlines, and all packets belonging to the same GOP has the same deadline. An important practical consequence of this fact is that EDF algorithm can be implemented at the application layer completely oblivious of the operation of the lower layer protocols. The only information required by EDF when implemented at the application layer is the acknowledgment of completion of GOP, which can be effectively inferred when the client sends a new HTTP-GET message for the subsequent GOP.

The operation of DASH based video streaming can be further conceptualized as follows. Each period of video streaming consists of a finite number of sub-segments, where each sub-segment belongs to one of the available representations. A segment is represented by $S(k, r)$, where k denotes the index of the segment and r denotes the corresponding video representation. The client begins the streaming period by first requesting the associated MDP file. The edge server acts as a *web proxy* for the client, requesting the MDP file from the video content delivery server on its behalf. A copy of the received MDP file is stored at the edge server, whereas another copy is forwarded to the client. The edge server utilizes the MDP files from all video streaming clients to provision the playout curves for each segment $S(k, r)$. Based on the received MDP file and the estimated network throughput, the client requests the first sub-segment among all available representations[9]. The client receives the data directly from the edge server. Once the download is complete, the client immediately requests the next sub-segment, and thus, acknowledging the complete and correct reception of the previous one. Note that the download times of each sub-segment may vary with respect to the size of the sub-segment, e.g., due to AVC encoding where each GoP may have different size, and the conditions of the channel between the edge server and the client.

[9]The smallest size of the sub-segment requested can be equal to the size of one GoP, which is what we assume in the subsequent sections.

Let $p_{i,k,r}(t)$ denote the playout curve of the segment $S(k,r)$ that is requested by client i. Hence, whenever client i requests a new sub-segment, which is a part of $S(k,r)$ during a period, the edge server generates the corresponding playout $p_{i,k,r}(t)$ to use in the scheduling algorithm, as such the generated playout curves are updated upon the arrival of ACK messages received in the form of HTTP-GET commands for subsequent sub-segments. This implies that the scheduling algorithm executed in the edge server does not need to trace the client buffer constantly, a critical feature to reduce the feedback load between the client and the edge server.

VI. Numerical Results

In this section, we demonstrate the performance of EDF as compared to round robin scheduling protocol under realistic channel and network conditions. All simulations are performed on NS-3. Recall that our protocol and its subsequent analysis is oblivious to the operation of lower layer networking stacks, but considers only whether the video packets are delivered to the end-user by their deadlines or not. An important question arises on how the performance of this application layer protocol is affected by the operation of the lower layer protocols, i.e., specifically TCP congestion control protocol, and under general channel loss models. Hence, in our simulations, we first considered a general Markov modulated channel model with packet loss varying among the states. We also considered both an ideal cross-layer mechanism, which provides perfect and instantaneous feedback to our application layer protocol, and a realistic TCP protocol that performs retransmissions and adjusts the congestion window size based on packet losses.

Although it can be easily implemented along with EDF algorithm, we do not consider the client-side quality selection mechanism for subsequent video segments in the simulations. That is, in our simulations, all subsequent segments (and sub-segments) are of the same quality. This allows us to more clearly demonstrate the improvement in the segment stalling probability provided by our proposed approach.

A. Experimental Setup

In the experiments, we use H.264/AVC video traces that are accessible on the internet [31], [32]. All video traces have CIF resolution (352 x 288) at 30 frames per second, frame configuration of 1 B frames in between I/P key pictures and Group of Pictures (GoP) size of 16 frames. The pool of videos considered in the simulations are named Tokyo Olympics, Silence of the Lambs, Star Wars IV, NBC News and Sony Demo. For each video file except Star Wars IV, we add video trace with quantization parameter (QP) of 10 and for Star Wars IV we add video traces with QP of 10 and 16 [10]. The segment size is assumed to be 10 seconds.

The data transmission channel between the edge server and a user is characterized by a data rate and the error model. For the error model, we use *RateErrorModel* class of NS-3. In the NS-3 environment, Rate Error Model is implemented under the transport layer hence TCP packets are dropped according to an underlying random variable distribution. In the literature, Packet Error Rate (PER) is considered in the range of $\left[10^{-2}, 10^{-4}\right]$ for the TCP simulations [34],[35]. Further, in [35] authors state that PER intervals $\left[10^{-3}, 10^{-4}\right]$, $\left[10^{-3}, 3\times10^{-3}\right]$, $\left[3\times10^{-3}, 10^{-2},\right]$ correspond to quality of service levels *excellent*, *good* and *satisfactory*, respectively. Hence, we consider a Markov modulated link model, where there are three states with packet drop probabilities $[0.001, 0.002, 0.005]$, respectively (each state corresponds to different quality of service level). The state transition probability matrix $\mathbf{\Gamma}$ is taken as:

$$\mathbf{\Gamma} = \begin{bmatrix} 0.3 & 0.6 & 0.1 \\ 0.2 & 0.6 & 0.2 \\ 0.1 & 0.6 & 0.3 \end{bmatrix}.$$

There is a state transition at every 0.5 seconds, and in between state transitions the packet loss probabilities remain constant.

Let λ_i (packets/sec) be the average rate of video packets generated for user i, which is calculated as the ratio of total size of the requested video file and the duration of the video. Also, let rt (bytes/sec) and ps (bytes/packet) be the fixed channel data rate and fixed packet size, respectively. Then, the *inverse* utilization rate ρ^{-1} is the ratio of the channel data rate and the cumulative video source rate, which is defined as,

$$\rho^{-1} = \frac{rt}{\left(\sum_{i=1}^{n} \lambda_i\right) ps}. \tag{13}$$

In the following, we only consider *underloaded* network scenarios, i.e., $\rho^{-1} > 1$, since those are the cases where the efficiency of a scheduling algorithm is more clearly observed.

B. Segment Stalling Probability Distribution

In this subsection, we analyze the distribution of the stalling events per segment when EDF and round-robing scheduling algorithms are employed. We consider a network with six users with each one requesting a different video file, e.g., Tokyo Olympics with QP=10, Silence of the Lambs with QP=10, Star Wars IV with QP=10, NBC news with QP=10, Sony Demo with QP=10, and Star Wars IV with QP=16. The duration of the simulation is taken as 10 seconds, which is also the duration of a segment. The experiment is repeated for 1000 times with different random seeds for the RateErrorModel class. However instead of using Markovian error rate model in the above we set the average packet loss rate to 0.2 for each user, and this corresponds to the packet loss experienced at the link layer. Whenever a packet is lost, we assume that there is a perfect and instantaneous feedback sent to the transmitter. Although packet loss rate of 0.2 is high for a realistic experiment, in this experiment we want to verify only our theoretical results and we want to increase randomness to observe larger scale of stalling events. We also note that that experiments, concerning system performance, are conducted according to the given Markovian model in the next subsection. The simulations are performed for ρ^{-1} values of $\{1.3, 1.35\}$. The results are summarized as histogram plots of the number of stalling events per segment for each ρ^{-1} value

[10]A quantization parameter is used to determine the quantization level of transform coefficients in H.264/AVC. An increase of 1 unit in the quantization parameter means an increase of quantization step size by approximately 12 percent, which in turn means 12 percent reduction in the video-rate [33].

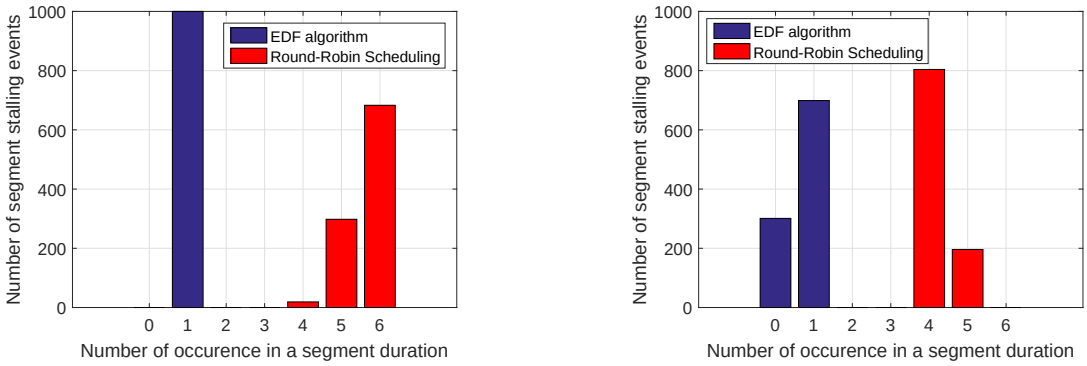

(a) $\rho^{-1} = 1.3$. (b) $\rho^{-1} = 1.35$

Fig. 5: The number of segment stallings.

in Fig. 5. Note that when $\rho^{-1} = 1.3$, users experience a single stalling event per segment duration, when EDF algorithm is employed. However, when round-robin algorithm is employed, approximately 70% of the time users experience six stalling events per segment and never less than four stalling events. When $\rho^{-1} = 1.35$, i.e., the network is less overloaded, the performance of EDF improves, with approximately 30% of the time users are experiencing no stalling events, and for the rest of the time they experience only one stalling event per segment. For the same case, round-robin improves its performance significantly also, with 80% of the time users experience four stalling events.

C. Average Number of Stalling Events per Minute

In this section, we investigate the average number of stalling events per minute with respect to the network utilization rate and video duration. The average number of stalling events per minute is defined as the ratio of the total number of segment stalling events of all users and the total number of users multiplied by the video duration. In our simulations, we assume that the clients have infinite size buffers used for storing incoming video packets. Whenever a stalling event occurs, the client freezes the display of the video through a certain prescribed time duration.

The performance of EDF algorithm is compared with a practical *round-robin* algorithm which is in-cognizant of the temporal properties of the video file. In particular, round-robin algorithm sends a fixed number of video packets to a client before serving another client. The round-robin algorithm is also implemented at the application layer, where the application process forwards a constant number (which is taken to be 30 in the simulations [11]) of video packets to the lower layer (TCP or an ideal transport layer), and awaits for the ACK for all of them. Once all packets are acknowledged, a client second in line is served in the same way. The process is repeated continuously until all video files are sent.

[11] As the number of packets increases the number of stalling events increases as well due to round robin waiting until all packets being acknowledged. If the number of packets decreases, then the number of stallings may also increase, but this time due to TCP overhead.

We first set the *initial buffer* duration to 0 second, which means that the client starts displaying the video immediately upon the arrival of the first video packet. The *rebuffer* duration is set to be 2 seconds, which means that the client freezes the display of the video during 2 seconds upon a stalling event. There are three clients, where each requesting the video files for Tokyo Olympics $QP = 10$, Star Wars IV $QP = 10$, NBC News $QP = 10$ respectively. We vary the length of the videos between 4 and 10 minutes, and for each duration we vary the value of inverse utilization rate ρ^{-1} from 1 to 1.5 in steps of 0.1. Each experiment scenario is repeated for 10 times with different random seeds for the random channel loss model. The results presented are the averages of these experiments.

As illustrated in Fig. 6, the average number of stalling events per minute decreases and ultimately approaches to zero as the data rate becomes much higher than the total video rate (i.e., as the inverse utilization rate increases). Note that the average number of stalling events per minute with EDF algorithm is at least 1.75 times lower than that of the round-robin algorithm, when TCP transport layer protocol is used. Also, as the inverse utilization rate increases, the average number of stalling events per minute decreases much rapidly for EDF algorithm. In fact, EDF algorithm can provide service with no stallings if the inverse utilization rate is more than 1.3 when implemented with TCP and 1.1 when implemented with an ideal transport layer. The round-robin algorithm cannot provide service with no stallings when the inverse utilization rate is less than 1.5 for both implementations (TCP and ideal transport layer). The round-robin algorithm is much more adversely affected by the TCP implementation than EDF, with its average stalling events per minute remain in the range of four stallings per minute even when inverse utilization rate is more than 1.5. We also observe that the video length has almost no effect on the outcome of the experiments for both algorithms.

The transport layer has significant impact on the performance. In the simulations, both algorithms are implemented at the application layer, and they wait until the transport layer queue has emptied before sending the packets for another user. Once there is a packet loss, the TCP time-out mechanism is provoked if an ACK is not received after *Retransmission Timeout (RTO)* duration. As per the specifications given in

RFC6298 [36], the minimum RTO duration is 1 second, even though this duration can be optimized to improve efficiency [37]. Note that during an RTO duration, no new packets are sent and the link becomes under-utilized. This affects not only the ongoing transmission, but also the subsequent GOP transmissions to other clients by limiting the amount of time that can be used to deliver video packets before their deadlines.

In the next set of simulations, we investigate the effect of rebuffer duration and video length. We implement our application layer scheduling policies together with TCP layer only. We set the initial buffer duration to 4 seconds, and the rebuffer durations are taken 2, 3, and 4 seconds. The duration of the video is $\{4, 6, 8, 10\}$ minutes. We performed the simulations for inverse utilization rates ρ^{-1} of 1 and 1.1. And each experiment scenario is repeated for 10 times with different random seeds for the random channel loss model then we take the average of them. Fig. 7 indicates that the average number of stalling events per minute stays approximately the same with increasing video length for a given rebuffer duration and ρ^{-1}. We also observe that the rebuffer duration is another important factor for decreasing the number of stalling events with its impact more prominent for larger ρ^{-1} values. Also note that the improvement in video stalling events is more significant when the rebuffering duration is increased from 2 seconds to 3 seconds, but this improvement gets smaller for higher rebuffer durations.

In Fig. 7, we depict the average number of stallings events per minute averaged over all clients, as well as for the client which has the highest the number of stallings among the three in the network. Although it is not identified as one of our main initial objective, we observe that EDF algorithm performs much more fairly than the round-robin algorithm in this aspect, too. The performance of the worst performing client, who requests the video stream with the highest source rate, is much closer to the average performance in the network as compared to that with the round-robin algorithm.

VII. Conclusions and Future Directions

This work introduces a DASH compatible network assisted control mechanism to be implemented at the edge server. We have first presented the notion of optimal scheduling policy to minimize the segment stalling event probability. Then, we have analytically proven that our proposed Earliest Deadline First algorithm minimizes the system-wise segment stalling probability when only average channel state information is available. We have demonstrated the efficacy of the algorithm with a realistic NS-3 simulation depicting its performance over an ideal transport layer with perfect feedback, as well as over a more common TCP transport layer. The simulations also demonstrate that EDF algorithm better utilizes the channel as compared to a naïve round robin policy.

We note that in our model the access point is oblivious to the instantaneous channel states, and only relies on ACK feedback taken in the form of HTTP-Get requests. This reduces the overhead and complexity of the implementation, but it may also affect its overall efficiency. In fact, there is a large body of work that investigates opportunistic scheduling algorithms by using instantaneous channel conditions. EDF algorithm is proven to be optimal when instantaneous channel information is not available; however, it is still an open problem to determine the best scheduling strategy minimizing the video stalling probability when partial or complete channel state information is available.

We also note that we aimed to minimize the maximum video stalling probability of all users. In some scenarios, other objectives such as minimizing the weighted average of individual user stalling probabilities, or minimizing the number of times a user experiences a stalling event per time interval may be more relevant. The optimal scheduling algorithms for different objectives can be considered as another interesting future research direction.

References

[1] Cisco, "Cisco visual networking : Forecast and methodology, 2013-2018," Jun. 2014, White Paper.

[2] Sandvine, "The global internet phenomena report: 2h 2014," Jun. 2014, White Paper.

[3] M. Claeys, S. Latre, J. Famaey, and F. De Turck, "Design and evaluation of a self-learning http adaptive video streaming client," *Communications Letters, IEEE*, vol. 18, no. 4, pp. 716–719, Apr. 2014.

[4] S. Garcia, J. Cabrera, and N. Garcia, "Quality-control algorithm for adaptive streaming services over wireless channels," *Selected Topics in Signal Processing, IEEE Journal of*, vol. 9, no. 1, pp. 50–59, Feb. 2015.

[5] C. Zhou, C.-W. Lin, X. Zhang, and Z. Guo, "A control-theoretic approach to rate adaption for dash over multiple content distribution servers," *Circuits and Systems for Video Technology, IEEE Transactions on*, vol. 24, no. 4, pp. 681–694, Apr. 2014.

[6] I. Sodagar, "The mpeg-dash standard for multimedia streaming over the internet," *MultiMedia, IEEE*, vol. 18, no. 4, pp. 62–67, Apr. 2011.

[7] T. Stockhammer, "Dynamic adaptive streaming over http –: Standards and design principles," in *Proceedings of the Second Annual ACM Conference on Multimedia Systems*, ser. MMSys '11. New York, NY, USA: ACM, 2011, pp. 133–144.

[8] R. Kuschnig, I. Kofler, and H. Hellwagner, "Evaluation of http-based request-response streams for internet video streaming," in *Proceedings of the Second Annual ACM Conference on Multimedia Systems*, ser. MMSys '11. New York, NY, USA: ACM, 2011, pp. 245–256.

[9] A. Begen, T. Akgul, and M. Baugher, "Watching video over the web: Part 1: Streaming protocols," *Internet Computing, IEEE*, vol. 15, no. 2, pp. 54–63, Mar. 2011.

[10] V. Joseph and G. de Veciana, "Nova: Qoe-driven optimization of dash-based video delivery in networks," in *INFOCOM, 2014 Proceedings IEEE*, Apr. 2014, pp. 82–90.

[11] A. Seetharam, P. Dutta, V. Arya, J. Kurose, M. Chetlur, and S. Kalyanaraman, "On managing quality of experience of multiple video streams in wireless networks," *Mobile Computing, IEEE Transactions on*, vol. 14, no. 3, pp. 619–631, Mar. 2015.

[12] S. Lederer, C. Müller, and C. Timmerer, "Dynamic adaptive streaming over http dataset," in *Proceedings of the 3rd Multimedia Systems Conference*, ser. MMSys '12. New York, NY, USA: ACM, 2012, pp. 89–94.

[13] D. Bethanabhotla, G. Caire, and M. Neely, "Adaptive video streaming for wireless networks with multiple users and helpers," *Communications, IEEE Transactions on*, vol. 63, no. 1, pp. 268–285, Jan. 2015.

[14] F. Fu and M. van der Schaar, "A systematic framework for dynamically optimizing multi-user wireless video transmission," *Selected Areas in Communications, IEEE Journal on*, vol. 28, no. 3, pp. 308–320, Apr. 2010.

[15] M. Li, Z. Chen, and Y.-P. Tan, "Scalable resource allocation for svc video streaming over multiuser mimo-ofdm networks," *Multimedia, IEEE Transactions on*, vol. 15, no. 7, pp. 1519–1531, Nov. 2013.

[16] H. Hu, X. Zhu, Y. Wang, R. Pan, J. Zhu, and F. Bonomi, "Proxy-based multi-stream scalable video adaptation over wireless networks using subjective quality and rate models," *Multimedia, IEEE Transactions on*, vol. 15, no. 7, pp. 1638–1652, Nov. 2013.

[17] X. Ji, J. Huang, M. Chiang, G. Lafruit, and F. Catthoor, "Scheduling and resource allocation for svc streaming over ofdm downlink systems," *Circuits and Systems for Video Technology, IEEE Transactions on*, vol. 19, no. 10, pp. 1549–1555, Oct. 2009.

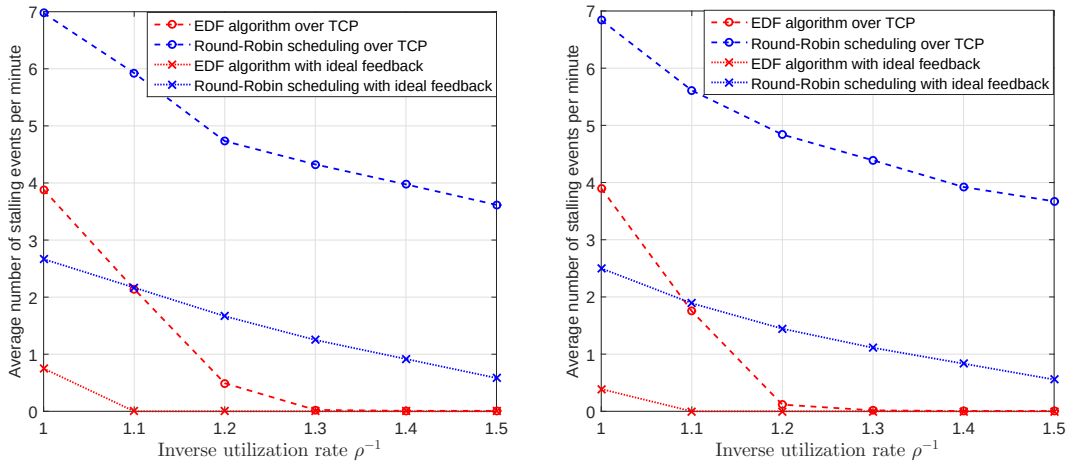
EDF algorithm over TCP
Round-Robin scheduling over TCP
EDF algorithm with ideal feedback
Round-Robin scheduling with ideal feedback
Average number of stalling events per minute
Inverse utilization rate ρ^{-1}

(a) Video duration is 4 minutes.

(b) Video duration is 6 minutes.

(c) Video duration is 8 minutes.

(d) Video duration is 10 minutes.

Fig. 6: Average number of stalling events per minute versus inverse utilization rate ρ^{-1}.

[18] S. Cicalo and V. Tralli, "Distortion-fair cross-layer resource allocation for scalable video transmission in ofdma wireless networks," *Multimedia, IEEE Transactions on*, vol. 16, no. 3, pp. 848–863, Apr. 2014.

[19] N. Freris, C.-H. Hsu, J. Singh, and X. Zhu, "Distortion-aware scalable video streaming to multinetwork clients," *Networking, IEEE/ACM Transactions on*, vol. 21, no. 2, pp. 469–481, Apr. 2013.

[20] M. Zhao, X. Gong, J. Liang, W. Wang, X. Que, and S. Cheng, "Qoe-driven cross-layer optimization for wireless dynamic adaptive streaming of scalable videos over http," *Circuits and Systems for Video Technology, IEEE Transactions on*, vol. 25, no. 3, pp. 451–465, Mar. 2015.

[21] A. Begen, T. Akgul, and M. Baugher, "Watching video over the web: Part 1: Streaming protocols," *Internet Computing, IEEE*, vol. 15, no. 2, pp. 54–63, Mar. 2011.

[22] I. Sodagar, "The mpeg-dash standard for multimedia streaming over the internet," *MultiMedia, IEEE*, vol. 18, no. 4, pp. 62–67, Apr. 2011.

[23] T. Stockhammer, "Dynamic adaptive streaming over http –: Standards and design principles," in *Proceedings of the Second Annual ACM Conference on Multimedia Systems*, ser. MMSys '11. New York, NY, USA: ACM, 2011, pp. 133–144.

[24] S. Akhshabi, A. C. Begen, and C. Dovrolis, "An experimental evaluation of rate-adaptation algorithms in adaptive streaming over http," in *Proceedings of the Second Annual ACM Conference on Multimedia Systems*, ser. MMSys '11. New York, NY, USA: ACM, 2011, pp. 157–168.

[25] T.-Y. Huang, N. Handigol, B. Heller, N. McKeown, and R. Johari, "Confused, timid, and unstable: Picking a video streaming rate is hard," in *Proceedings of the 2012 ACM Conference on Internet Measurement Conference*, ser. IMC '12. New York, NY, USA: ACM, 2012, pp. 225–238.

[26] S. Akhshabi, L. Anantakrishnan, A. C. Begen, and C. Dovrolis, "What happens when http adaptive streaming players compete for bandwidth?" in *Proceedings of the 22Nd International Workshop on Network and Operating System Support for Digital Audio and Video*, ser. NOSSDAV '12. New York, NY, USA: ACM, 2012, pp. 9–14.

[27] L. De Cicco and S. Mascolo, "An adaptive video streaming control system: Modeling, validation, and performance evaluation," *Networking, IEEE/ACM Transactions on*, vol. 22, no. 2, pp. 526–539, Apr. 2014.

[28] S. Akhshabi, L. Anantakrishnan, C. Dovrolis, and A. C. Begen, "Server-based traffic shaping for stabilizing oscillating adaptive streaming players," in *Proceeding of the 23rd ACM Workshop on Network and Operating Systems Support for Digital Audio and Video*, ser. NOSSDAV '13. New York, NY, USA: ACM, 2013, pp. 19–24.

[29] J. Jiang, V. Sekar, and H. Zhang, "Improving fairness, efficiency, and stability in http-based adaptive video streaming with festive," *Networking, IEEE/ACM Transactions on*, vol. 22, no. 1, pp. 326–340, Feb. 2014.

[30] M. L. Puterman, *Markov Decision Processes: Discrete Stochastic Dynamic Programming*, 1st ed. New York, NY, USA: John Wiley & Sons, Inc., 1994.

[31] G. Van der Auwera, P. David, and M. Reisslein, "Traffic and quality characterization of single-layer video streams encoded with the h.264/mpeg-4 advanced video coding standard and scalable video coding extension," *Broadcasting, IEEE Transactions on*, vol. 54, no. 3, pp. 698–718, Sep. 2008.

[32] P. Seeling, M. Reisslein, and B. Kulapala, "Network performance evaluation using frame size and quality traces of single-layer and two-layer video: A tutorial," *Communications Surveys Tutorials, IEEE*, vol. 6, no. 3, pp. 58–78, Third 2004.

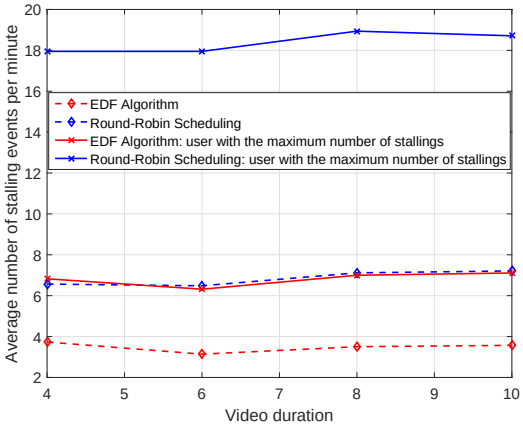
EDF Algorithm
Round-Robin Scheduling
EDF Algorithm: user with the maximum number of stallings
Round-Robin Scheduling: user with the maximum number of stallings
Average number of stalling events per minute
Video duration

(a) Rebuffer duration is 2 seconds, and $\rho^{-1} = 1$.

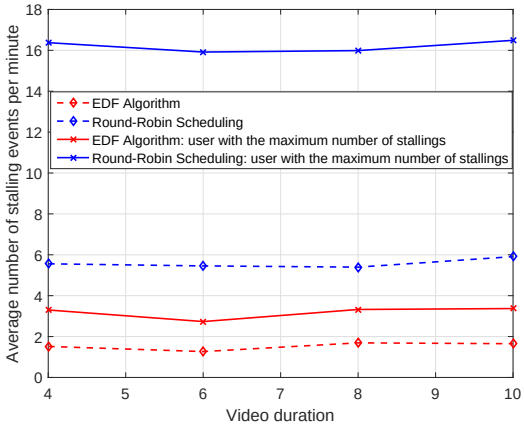
EDF Algorithm
Round-Robin Scheduling
EDF Algorithm: user with the maximum number of stallings
Round-Robin Scheduling: user with the maximum number of stallings
Average number of stalling events per minute
Video duration

(b) Rebuffer duration is 2 seconds and $\rho^{-1} = 1.1$.

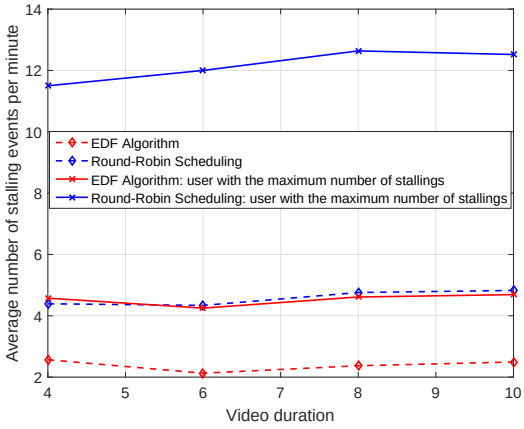
EDF Algorithm
Round-Robin Scheduling
EDF Algorithm: user with the maximum number of stallings
Round-Robin Scheduling: user with the maximum number of stallings
Average number of stalling events per minute
Video duration

(c) Rebuffer duration is 3 seconds and $\rho^{-1} = 1$.

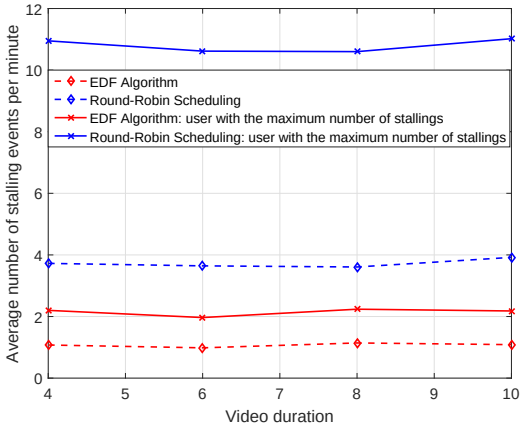
EDF Algorithm
Round-Robin Scheduling
EDF Algorithm: user with the maximum number of stallings
Round-Robin Scheduling: user with the maximum number of stallings
Average number of stalling events per minute
Video duration

(d) Rebuffer duration is 3 seconds and $\rho^{-1} = 1.1$.

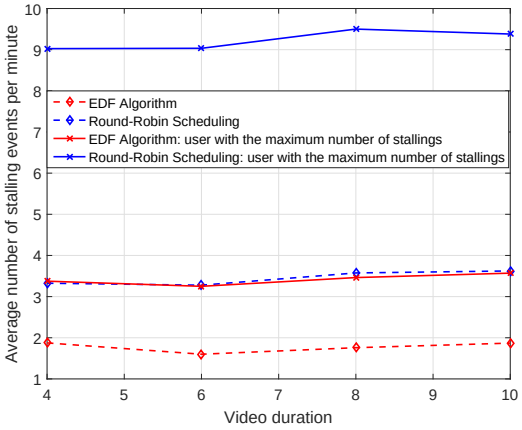
EDF Algorithm
Round-Robin Scheduling
EDF Algorithm: user with the maximum number of stallings
Round-Robin Scheduling: user with the maximum number of stallings
Average number of stalling events per minute
Video duration

(e) Rebuffer duration is 4 seconds and $\rho^{-1} = 1$.

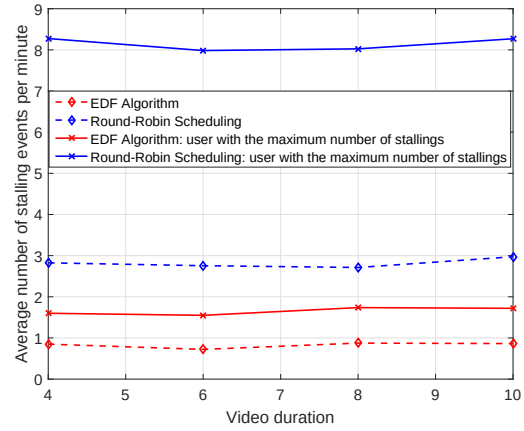
EDF Algorithm
Round-Robin Scheduling
EDF Algorithm: user with the maximum number of stallings
Round-Robin Scheduling: user with the maximum number of stallings
Average number of stalling events per minute
Video duration

(f) Rebuffer duration is 4 seconds and $\rho^{-1} = 1.1$.

Fig. 7: Average number of stalling events per minute with respect to video duration and rebuffer duration.

[33] T. Wiegand, G. Sullivan, G. Bjontegaard, and A. Luthra, "Overview of the h.264/avc video coding standard," *Circuits and Systems for Video Technology, IEEE Transactions on*, vol. 13, no. 7, pp. 560–576, Jul. 2003.

[34] S. Gangadhar, T. A. N. Nguyen, G. Umapathi, and J. P. G. Sterbenz, "Tcp westwood(+) protocol implementation in ns-3," in *Proceedings of the 6th International ICST Conference on Simulation Tools and Techniques*, ser. SimuTools '13. ICST, Brussels, Belgium, Belgium: ICST (Institute for Computer Sciences, Social-Informatics and Telecommunications Engineering), 2013, pp. 167–175.

[35] O. I. S. Aderemi A. Atayero and Y. A. Ivanov, "IAENG transactions on engineering technologies," in *Modeling, Simulation and Analysis of Video Streaming Errors in Wireless Wideband Access Networks*, H. K. Kim, S. Ao, and B. B. Rieger, Eds. Dordrecht: Springer, 2013, ch. 2, pp. 15–28.

[36] V. Paxson, M. Allman, J. Chu, and M. Sargent, "Computing TCP's Retransmission Timer," RFC 6298 (Proposed Standard), Internet Engineering Task Force, Jun. 2011. [Online]. Available: http://www.ietf.org/rfc/rfc6298.txt

[37] A. Kesselman and Y. Mansour, "Optimizing tcp retransmission timeout," in *in ICN 05: Proceedings of The 4th International Conference on Networking, 2005*, 2005, pp. 133–140.